Journal of Power Sources 187 (2009) 393–399

Contents lists available at ScienceDirect

Journal of Power Sources

journal homepage: www.elsevier.com/locate/jpowsour

Development of a tubular microbial fuel cell (MFC) employing a membrane electrode assembly cathode

Jung Rae Kim[a], Giuliano C. Premier[a,*], Freda R. Hawkes[b], Richard M. Dinsdale[b], Alan J. Guwy[b]

[a] Sustainable Environment Research Centre (SERC), Faculty of Advanced Technology, University of Glamorgan, Pontypridd, Mid-Glamorgan CF37 1DL,UK
[b] Sustainable Environment Research Centre (SERC), Faculty of Health, Sport and Science, University of Glamorgan, Pontypridd, Mid-Glamorgan CF37 1DL, UK

ARTICLE INFO

Article history:
Received 27 June 2008
Received in revised form 27 October 2008
Accepted 1 November 2008
Available online 17 November 2008

Keywords:
Microbial fuel cell
Membrane electrode assembly
Tubular
Impedance Spectroscopy
Ion exchange membrane
Electro-osmotic drag

ABSTRACT

Tubular microbial fuel cells (MFC) with air cathode might be amenable to scale-up but with increasing volume a mechanically robust, cost-effective cathode structure is required. Membrane electrode assemblies (MEA) are investigated in a tubular MFC using cost-effective cation (CEM) or anion (AEM) exchange membrane. The MEA fabrication mechanically combines a cathode electrode with the membrane between a perforated cylindrical polypropylene shell and tube. Hydrogel application between membrane and cathode increases cathode potential by ~100 mV over a 0–5.5 mA range in a CEM-MEA. Consequently, 6.1 W m^{-3} based on reactor liquid volume (200 cm^3) are generated compared with 5 W m^{-3} without hydrogel. Cathode potential is also improved in AEM-MEA using hydrogel. Electrochemical Impedance Spectroscopy (EIS) to compare MEA's performance suggests reduced impedance and enhanced membrane–cathode contact area when using hydrogel. The maximum coulombic efficiency observed with CEM-MEA is 71% and 63% with AEM-MEA. Water loss through the membrane varies with external load resistance, indicating that total charge transfer in the MFC is related to electro-osmotic drag of water through the membrane. The MEA developed here has been shown to be mechanically robust, operating for more than six month at this scale without problem.

1. Introduction

Microbial fuel cells (MFCs) have been studied for sustainable energy generation and wastewater treatment technology [1–4]. Cost-effective reactor designs and materials are required for field scale applications. Unlike a conventional bioreactor, MFCs consist of compartments or elements for electrochemical reactions, including an anode chamber, a cathode and often an ion exchange membrane and a chamber associated with the cathode. These segmented parts make MFCs difficult to scale up in an optimal design configuration. There have been efforts to make simple reactor configurations that remove the membrane and cathode chamber, e.g. using an air cathode [5–7].

An air cathode without a membrane, sustained using oxygen delivered by natural convective movement of air and diffusion, is likely to be the most cost-effective cathode system as compared with alternatives that involve aeration energy or use of non-sustainable catholytes, e.g. hexacyanoferrate and permanganate [5,6,8,9]. However, without a proton exchange membrane there is a greater possibility of substrate loss and biofouling on the cathode by increased oxygen intrusion, which can sustain aerobic biological activity. This could be especially true with complex substrates and/or wastewaters that are degraded by different trophic groups, because the oxic/anoxic interface on air cathodes can be a favourable environment for bacterial consortia. Therefore, biofilms on the cathodes might inhibit the cathodic reduction reaction [10–12]. Porous barriers such as J-cloth or nanoporous filter material have been suggested to decrease oxygen diffusion and increase coulombic efficiency [7,13]. However in a larger scale reactor (e.g. a vertical tubular reactor), such materials may not be able to resist leakage caused by hydrostatic pressure and mechanical strain.

Membrane electrode assembly (MEA) configurations have been designed and widely investigated in chemical fuel cells [14]. Although a MEA has been studied in MFCs using hot pressed Nafion/cathode electrode assemblies [5,15], its performance in MFCs did not deliver an improvement compared with those of membrane-less MFCs. Furthermore, the expense of Nafion exchange membrane is a barrier to scale-up and development. Cost-effective anion and cation exchange membranes other than Nafion have been investigated in MFCs, where these membranes can both lead to effective MFC operation [16,17]. These supported heterogeneous membranes with polyvinylidenefluoride (PVDF) binder have been reported as being unsuitable for hot pressing as they are not heat weldable to other than high cost PVDF forms [18] for MEA

* Corresponding author. Tel.: +44 1443 482333; fax: +44 1443 482169.
E-mail address: gcpremier@glam.ac.uk (G.C. Premier).

0378-7753/$ – see front matter © 2008 Elsevier B.V. All rights reserved.
doi:10.1016/j.jpowsour.2008.11.020

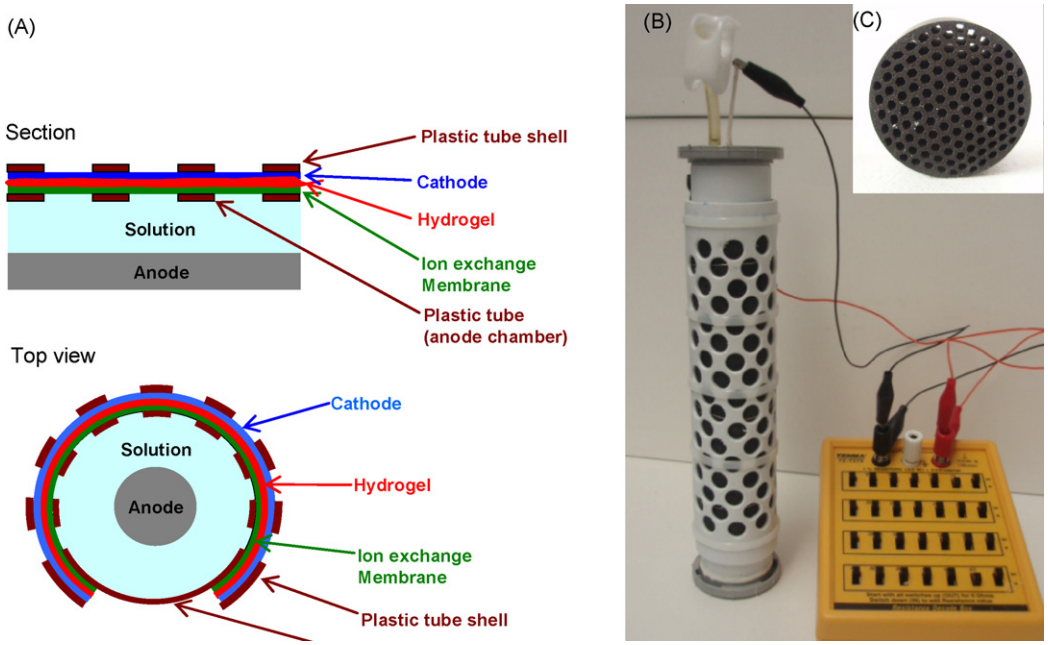

Fig. 1. Membrane electrode assembly (MEA) structure schematic diagram (A), photograph of a tubular membrane electrode assembly MFC (B) and photograph of the cross sectional view of the monolithic carbon anode (C).

assemblies. The MEA plays a key role as an electrolyte medium for ion transport and a barrier to avoid direct contact between fuel and oxygen. Therefore, development of cost-effective MEA fabrication for MFCs is required.

In this study we developed a low cost tubular MFC reactor, which might be scalable by longitudinal extension, employing a MEA cathode which combined a cost-effective polymer based ion exchange membrane and a cathode electrode. An hydrogel was investigated in order to improve contact between the cathode and the membrane. The behaviour of the MEA was studied by monitoring the electrical output of the MFCs, by using Electrochemical Impedance Spectroscopy (EIS) [19] and by investigating the net water loss through the MEA structure.

2. Materials and methods

2.1. MFC configuration and operation

The tubular MFC reactors (Fig. 1) consisted of a cylindrical polypropylene tube with a monolithic activated carbon anode and either a cation exchange membrane or an anion exchange membrane (CMI-7000 and AMI-7001 respectively, Membrane International Inc., NJ, USA), assembled with a cathode. The polypropylene tube, 23 cm long and 3.6 cm diameter, had equi-spaced 1 cm diameter holes at 2 cm intervals and the region with holes was covered by a 19 cm × 12 cm membrane. The multi-channel monolith carbon (Novacarb^{TM} MAST Carbon Ltd., Guildford, UK), was a carburized prismatic polymeric extrusion 10 cm long, 2 cm diameter, with longitudinal hexagonal channels (Fig. 1C), heat treated at 1600 °C to increase electrical conductivity. The anode was transferred between MFCs with different MEA configurations as described and placed concentrically in the polypropylene tube. The empty bed volume of the anode chamber (with anode in place) was 200 cm^3 and the reactor was operated vertically. The cathode electrode was exposed to air on its outer surface, as well as being in contact with the membrane (Fig. 1). Anode and cathode electrodes were connected to a resistive external load (1000 Ω during start-up and 150 Ω thereafter except during evaluation of power density and EIS).

The MFC reactors were initially inoculated with anaerobic digester sludge (Cog Moors Sewage Treatment Works, Cardiff, UK), in the ratio 1:10 with media containing acetate (40 mM), phosphate buffer (50 mM, pH 7.0) and nutrients [16]. The anode was enriched while connected to a 1000 Ω external resistance. After 1 week and 2 weeks, half of the anode chamber content was removed and replaced with fresh acetate containing medium (40 mM). Thereafter the total anode contents were replaced with fresh medium weekly, or more frequently during assays. At start-up the voltage gradually increased over the two weeks and stabilized at 0.47–0.48 V and remained *quasi* static until the testing regime started. The MFC was operated at 26 ± 2 °C.

Four MEA configurations were tested (CEM-MEA, AEM-MEA with/without gel). They were tested against the same monolithic carbon anode which was transferred between them and upon which an exoelectrogenic biofilm had been established. While not occupied by the monolithic test anode, a rolled carbon veil anode of similar proportions and experimental history was used to maintain hydration and functional comparability and integrity of the MEAs. The CEM-MEA and AEM-MEA without gel were operated for more than 6 months, after which gel was applied and the systems continued in operation in excess of a month further. This testing presented in Section 2.3 was conducted in one week either side of this changeover. Therefore, EIS, anode, cathode, and whole cell potential were measured using the separate MEA configurations, with the same monolith carbon anode. Using the same enriched anode electrode removed the likelihood of MFC performances being affected by differences in anode performance.

2.2. Membrane electrode assembly fabrication

The membrane electrode assembly consisted of the ion exchange membrane and carbon cloth cathode electrode containing 0.5 mg cm^{-2} Pt. Pt powder was mixed with carbon black (Vulcan XC-72R, Cabot Co. NC, USA) using Nafion (5% perfluorinated ion-exchange resin, Sigma–Aldrich, MO, USA) as binder [20]. Where

used, hydrogel (ECG gel, Camcare, Cambridgeshire UK) was evenly applied between the membrane and cathode electrode in order to increase hydration of the cathode and the contact area between the cathode and membrane. The MEA (228 cm^2) was wrapped and attached around the polypropylene tube (anode chamber) using double sided tape (3M™ 4950 VHB™ tape, MN, USA). Another longitudinally split polypropylene tube with holes of the same spacing and diameter as the inner tube formed a shell which was clipped around the outside of the cathode in order to hold the cathode onto the membrane while giving the assembly mechanical strength. The performance of the MEA without hydrogel was compared with the MEA with hydrogel. Normally, the hydrogel MEA was dried in air for a day before use in the MFC. One EIS test investigated a CEM-MEA with fresh hydrogel in an undried state.

2.3. Analyses

The voltage across the load was monitored by a computer based data logging system (LabVIEW™) at 1 min intervals. The cell, anode and cathode potential measurements were conducted using a Solartron Instruments (Farnborough, UK) 1287 electrochemical interface with an Ag/AgCl reference electrode while monitoring and datalogging the dynamic potential using LabVIEW™ on a personal computer with a multi-purpose Input/Output card (National Instruments, Newbury, UK). The Galvanostatic method (CorrWare 2™, Scribner Associate Inc., NC) which applies constant current and monitors potential as a function of time was used. Each cell potential was measured after 20 min intervals to allow the voltage to settle. Before each MEA configuration was tested, the anode contents were replaced with fresh media containing acetate (40 mM) and the MFC allowed to stabilize over at least 12 h. Power density and coulombic efficiency (CE) were calculated as previously described [21]. The CEs were obtained from a series of fed batch cycles containing different initial acetate concentrations (0.4–3.6 mM). The voltage was generated from the specific amount of acetate added, which decreased in time, to below approximately 10 mV at which point acetate was considered to have been depleted. We determined the experimental coulombs of electrical generated by integrating the voltage against time curves (*Ce*). This was then compared with the theoretically available coulombs from the acetate dosed in the batch fed cycle (*Ct*). The coulombic efficiencies were calculated according to: CE = *Ce*/*Ct*. The CE would be reduced if measured at about 40 mM acetate concentrations, if determined by the same methodology. The long period required to deplete the acetate would allow increase oxygen intrusion through the membrane and reduced pH through metabolic activity, both tending to reduce CE.

The MEA performance was analyzed by EIS using a Solartron Analytical (Farnborough, UK) 1287 Electrochemical Interface and a 1255 Impedance Phase Analyzer, connected to a personal computer equipped with CoreWare™, CoreView™, ZPlot™ and ZView™. The electrochemical impedance spectra were recorded over a frequency range of 1 mHz to 300 kHz, which includes the range considered significant for biological systems presented in [22] and the amplitude of the modulating sinusoidal voltage was 15 mV. EIS spectra were considered in the Nyquist domain and fitted to equivalent circuit models.

EIS was conducted on the open circuit MFCs and it was expected that with differing MEA configurations, using the same anode, this would discriminate between the effects on equivalent circuit functional elements when using anion exchange membrane (AEM) and cation exchange membrane (CEM), with and without hydrogel in the MEA. The equivalent circuit elements represented electrolyte resistance (*Re*) and charge transfer and/or polarization resistance (*Ret*). A Constant Phase Element (*CPEdl*, where $Z = 1/A_o(j\omega)^n$) was used to represent the double layer capacitance as it was expected to be distributed by virtue of the rough, complex and elongated shape of the electrode. Also, the system was assumed to be supported and therefore it would be possible to neglect the migration term in the Nernst-Planck equation, which then reduces to Fick's first law of diffusion, as presented by Franceschetti et al. [23]. Thus Generalized Finite Warburg (GFW) elements, as presented in Table 1, were employed to represent diffusion processes in the MFCs. These elements were arranged into a Randles and Ershler model configuration similar to that reported in [22], yielding models A and B (Table 1). The AEM and CEM, with and without hydrogel (in its dried condition) could be compared directly, as the equivalent circuit model structures were identical. The GFW element was altered to adequately represent the CEM-MEA with undried hydrogel included.

Equivalent circuit models were fitted to the data using the complex nonlinear fitting functionality of ZView2™, with weighting normalized according the impedance magnitude. The open circuit GFW element (Table 1) provided a better fit in all but one of the cases of MEA considered. The MEA using undried hydrogel was better represented by the shorted GFW used as a Finite Length Warburg element (i.e. GFW with the exponent *p* fixed at 0.5). In Table 1, the length l_e is the notional electrode thickness for diffusion, *D* is the diffusion coefficient. $C_{limiting}$ and $R_{limiting}$ are respectively the capacitance and resistance to which the open and short circuited versions of the Generalized Finite Warburg elements will tend at low frequencies. Finally, a small inductance (*L*) was included, but was of marginal interest as it occurred at high frequencies ~>10 kHz.

The accumulated net water loss was considered in the case of the CEM-MEA with hydrogel and was determined by weighing the MFC reactor during its operation and comparing this with its initial weight.

3. Results

3.1. Cell potentials and power density

The performance of the MEA was evaluated by the potential–current response (Fig. 2). The cathode potential of the MEA employing CEM with hydrogel was about 100 mV higher than the MFC without hydrogel over the whole range of current (Fig. 2A). The maximum power density from the MFC employing hydrogel and the MFC without hydrogel were 6.1 W m^{-3} and 5.0 W m^{-3} of anode chamber liquid volume at 4 mA of current, respectively (Fig. 2B). The increased cell potential and power density is clearly due to improved cathode potential as the anode potential was essentially the same. The power density was maintained over 6 months without any deterioration of performance. The MEA using AEM showed significantly increased cathode and cell potential when hydrogel was used (Fig. 3A). The effects of hydrogel were more pronounced in the AEM-MEA, with the anode potentials deviation at higher currents over ~2.5 mA, probably as a result of polarization. The cathode potentials however, deviated over the entire current range apart from open circuit, which is probably due to the availability for transference of anionic species through or from the hydrogel. The maximum power density with the MEA using AEM was 4.9 W m^{-3} at 3.5 mA of current (Fig. 3B).

3.2. Coulombic efficiency

The coulombic efficiencies of the MEA employing cation exchange membrane were 55–71% (Fig. 4) across a range of acetate concentrations from 0.4 mM to 3.6 mM. The maximum CE with anion exchange membrane was 63% at 3.6 mM acetate.

Table 1
Model parameters derived from complex fitting (with ZView2™) and equivalent circuit model of the tubular MEA MFC.

Data set	Electrolyte resistance	Charge transfer and/or polarization resistance	Generalized Finite Warburg[a] – Diffusion Model (*Wd*) [open circuit (Wo – A) and short circuit (Ws – B)]		Constant phase element[b] – double layer capacitance		High frequency inductance	Weighted sum squared error fit	Equivalent Circuit Model
	Re [Ω]	*Ret* [Ω]	*AWo or AWs*	*τ* [s]	*p*	$A_o \times 10^{-3}$	*n*	*L* [μH]	–	–
AEM with gel	13.11	0.69	12.84	21.85	0.38337	16.86	0.45190	0.65	0.145	A
AEM without gel	11.56	5.56	67.85	36.99	0.33799	14.57	0.39143	0.69	0.043	A
CEM with gel	9.148	0.23	7.623	13.95	0.40574	56.34	0.50480	0.83	0.417	A
CEM without gel	5.266	0.26	8.881	14.56	0.41417	57.90	0.48680	1.29	0.759	A
CEM with gel (undried)	5.765	0.41	33.6	85.2	0.500 (fixed)	245.28	0.38220	0.91	0.366	B

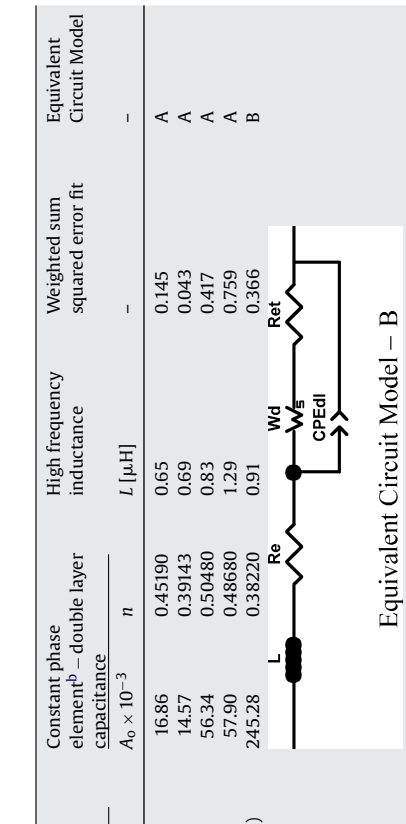

[a] $Z_{Wo} = A_{Wo}.ctnh(j\tau\omega)^p/(j\tau\omega)^p$ and $Z_{Ws} = A_{Ws}.\tan h(j\tau\omega)^p/(j\tau\omega)^p$ Where $\tau = l_e^2/D$ and $A_{Wo} = \tau/C_{limiting}$ or $A_{Ws} = R_{limiting}$ where l_e represents the electrode thickness and D represents the diffusion coefficient. Presented similarly in [34].
[b] $Z_{CPE} = \frac{1}{A_o(j\omega)^n}$ where $A_o = |Z|$ at $\omega = 1\ rad\ s^{-1}$.

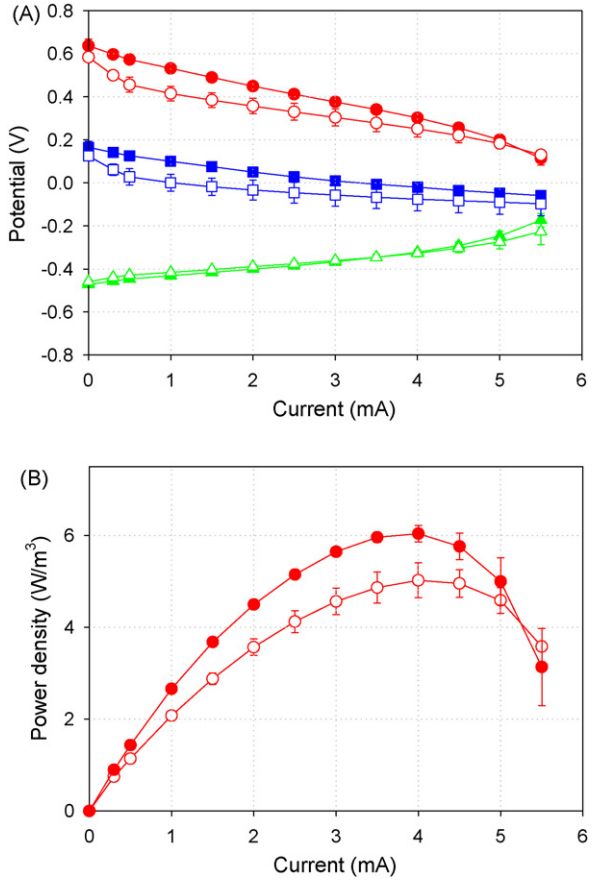

Fig. 2. Comparison of potential and power density of MEA MFC employing cation exchange membrane (CEM) as a function of power density normalized by reactor volume (filled symbols: MEA with applied hydrogel, open symbols: MEA without hydrogel). (A) electrode potential (cell potential: circle, cathode potential: rectangle, anode potential: triangle), (B) power density based on empty bed volume of anode chamber (error bar based on averages measured in duplicate analysis).

The higher CE obtained at acetate concentrations over 1 mM could be attributed to higher substrate concentrations lowering overpotential caused by mass transport limitation on the anode surface.

3.3. Electrochemical Impedance Spectroscopy

The open circuit EIS on the MFCs using hydrogel and CEM or AEM in an MEA, are presented in the Nyquist (Fig. 5) domain. Considering first the four MEAs described by model A (Table 1), the notional electrolyte resistance (*Re*), which would include the membrane and hydrogel, was higher for AEM than for CEM and the use of hydrogel tended to increase this resistance. The charge transfer and/or polarization resistance (*Ret*) was below ~0.7 Ω, apart from the case with AEM without hydrogel (5.56 Ω), indicating that the charge transfer was affected by membrane selection and hydrogel use. Particularly, the use of hydrogel with AEM (which at the time of the EIS, had been in use for 4 months on the tubular MFC), reduced *Ret* by a factor of 8, and is believed to have caused the increase in power density from AEM without, to AEM with hydrogel (Fig. 3). The hydrogel had the effect of reducing $A_{Wo} = \tau/C_{limiting} = (l_e^2/D)/C_{limiting}$ (again, more so with the AEM than the CEM), In the case of CEM, inclusion of hydrogel marginally reduced τ (14.56–13.95 s) and A_{Wo} (8.881–7.623 Ω), indicating that it is plausible that a contribution at least, did not stem only from increased capacitance $C_{limiting}$, but was also due to

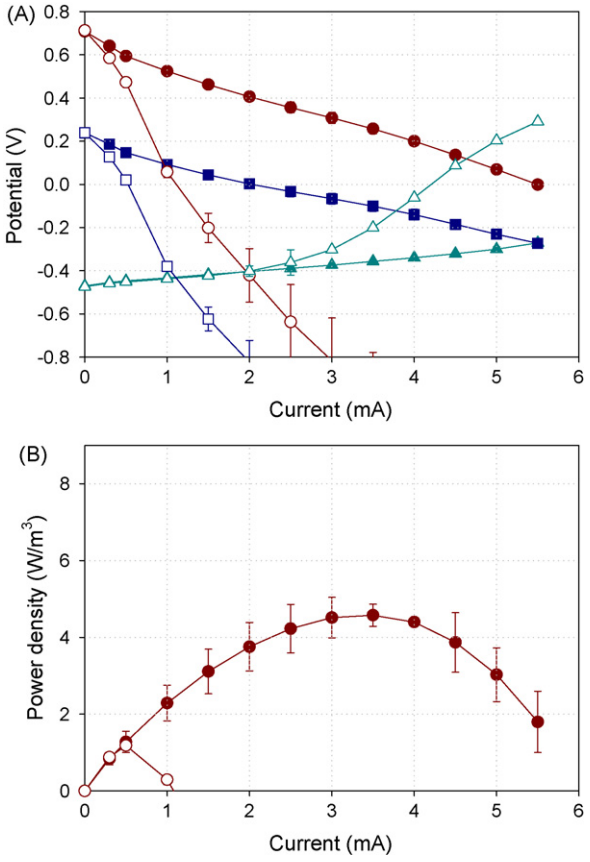

Fig. 3. Comparison of potential and power density of MEA MFC employing anion exchange membrane (AEM) as a function of power density normalized by reactor volume (MEA with applied hydrogel is filled symbol and MEA without hydrogel is open symbol). (A) Electrode potential (circle is cell potential, rectangle is cathode potential, and triangle is anode potential), (B) power density based on empty bed volume of anode chamber (error bar based on averages measured in duplicate analysis).

increased diffusion coefficient D. This tends to indicate a coupling in the model, between anodic and cathodic mass transfer of charged particles.

In the case of AEM, the reduction of τ (36.99–21.85 s) and A_{Wo} (67.85–36.99 Ω) were considerably larger, and may be reflected in the MFC's improved cathode performance. Again, improvement is

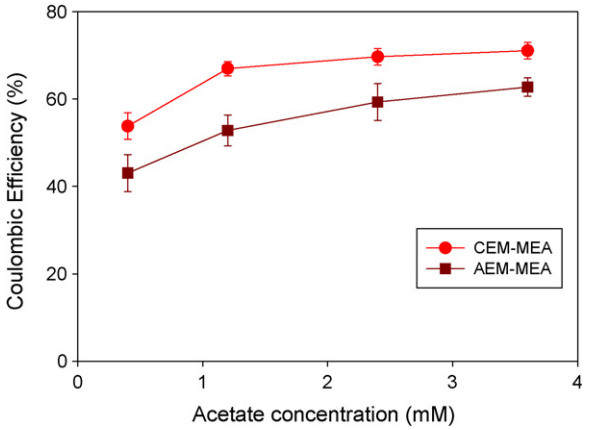

Fig. 4. Coulombic efficiency of membrane electrode assembly MFC using cation exchange membrane (CEM) and anion exchange membrane (AEM) according to acetate concentration (error bar based on averages measured in duplicate analysis).

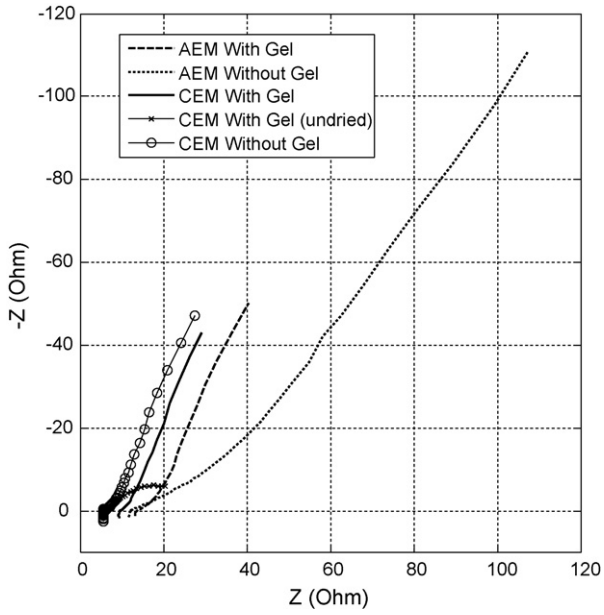

Fig. 5. Nyquist plots showing differences caused by differing MEA construction and membrane type. Impedance spectra recorded using a single sine wave modulation of 15 mV amplitude.

likely to have diffusional and capacitive contributions. The double layer capacitance represented by the CPE element was not thought to have been greatly affected by the dried hydrogel, but did show a slight increase in A_o for the AEM and reduction in CEM-MEAs, with a slight increase in the exponent n in both cases (indicating an alteration in the distributive capacitive morphological features of the cathode electrode, marginally toward a lumped or ideal capacitance).

In considering CEM with undried hydrogel, it was necessary to use a Finite Length Warburg element diffusion model to adequately represent and fit the data. When the water content of the hydrogel was reduced by drying, an increase in *Re* was observed, while the *Ret* was reduced. However, some uncertainty exists in this regard as the diffusion models were not the same between the undried and dried hydrogel tests. From Fig. 5 it is evident that fresh undried hydrogel in the CEM reduced $|Z|$ and phase lag at low frequency, which may indicate a change from capacitance limiting to resistance limiting behaviour at low frequencies (toward 1 mHz) in the MFC. The undried hydrogel is seen to have a discernable effect on the diffusion and double layer capacitance models, not least by altering the structure to Model-B (Table 1).

3.4. Electro-osmotic drag through membrane

The medium in the anode chamber makes contact with the MEA transferring various dissolved ionic species and water. During MFC operation, these ions migrate through the membrane taking with them water molecules by electro-osmotic drag as has been investigated in chemical fuel cells [14,24,25]. Accumulated net water loss through the membrane varies simultaneously with total charge transfer, according to external load resistance (Fig. 6). The MEA type cathode electrode studied employs a large aerobic/anaerobic interface around the anode chamber as compared with configurations in the literature [8,26,27], therefore the transmembrane pressure differential and natural evaporation from the membrane are likely reasons for water loss from the reactor in open circuit.

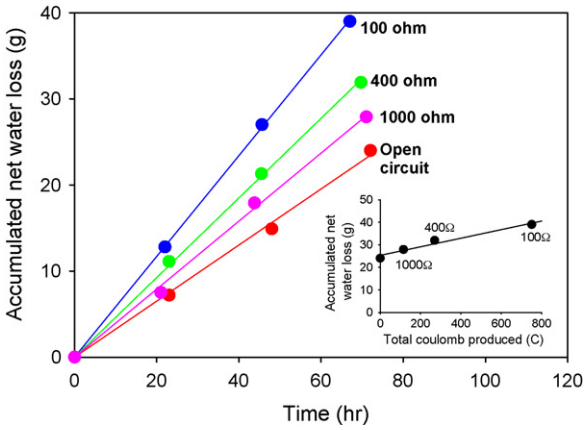

Fig. 6. Accumulated net water loss through MEA using different external resistance according to time. The inset graph shows the relationship between net water loss and total coulomb produced during 72 h of MFC operation using each resistance.

4. Discussion

The membrane has been used as a separator for aerobic/anerobic compartments as well as an ion exchange mediator in the MFCs. Although membrane-less MFCs have been investigated in order to eliminate overpotentials induced by a membrane, low fuel efficiency and oxygen intrusion are concerns [5,26]. It has been suggested that a membrane electrode assembly might not work efficiently in MFCs due to inadequate wetting and loss of catalytic activity [5,28]. This work shows that a mechanically combined low cost ion exchange membrane and cathode electrode supports electrochemical reactions for MFCs with sufficient hydration of the cathode to facilitate oxygen reduction.

Dimensional instability of ion exchange membrane by water uptake is an intrinsic characteristic of membranes which have hydrophilic and hydrophobic functional groups [14]. This deformation results in deterioration of catalytic activity by decreasing the contact area between the membrane and cathode electrode in MEA structure. Work on chemical fuel cells has introduced hot pressed fabrication of MEA using Nafion and cathode [14]. However it is difficult to fabricate MEAs using other polymer based membranes where thermal denaturation and degeneration may occur. The feasibility of fabricating high performance MEAs for MFCs was studied with a view to further develop them for scale-up, which might be achieved by maintaining the cross section and extending the MFCs longitudinally. In this report, we overcame this drawback by using an additional split plastic tube shell to give mechanical stability by pressing the cathode electrode onto the membrane, and by applying an intermediate layer of hydrogel. We showed that hydrophilic hydrogel improved MFC performance probably by increasing hydration and contact area between the membrane and cathode, filling the gaps caused by their textural topology and deformation. The effect of hydrogel was more significant when anion exchange membrane was used, probably due to different ion exchange characteristics.

The results presented in Figs. 2 and 3 indicate that the ion exchange characteristics of membranes affect the cathode potential, as does the improved charge transfer effect of hydrogel between membrane and cathode. It was also evident that the hydrogel improved power density by increasing cathode potential. The cathode and anode potential reported here were similar to those found by Zuo et al. [4], who used 23–36 ml of reactor volume. The power density obtained here was low as compared with recent reports [6,27]. However these also used significantly smaller reactors and the power density normalized by reactor volume does not provide information on reactor size which is an important factor for scale-up. Therefore, sacrificial power loss would be expected in larger MFC reactors as scale-up normally results in increased overpotential and mass transport limitation. The coulombic efficiency of the MEA MFCs employing ion exchange membranes is comparable with that of single chamber MFCs using J-cloth [13] or membrane-less MFC [5,16,29], but it should be noted that in our work a significantly larger membrane area or aerobic/anaerobic interface was used.

There are clear indications of changes in the impedance spectra when employing the different configurations of MEA presented and in order to interpret the changes equivalent circuit models have been proposed. The tubular design of the MFCs and the monolithic carbon anode investigated meant that the distributed nature of the double layer capacitance of the system components and mass transfer effects required the used of a Constant Phase Element and GFW element respectively, to adequately represent these functions. However, it was possible to reveal the parameters representing notional sources of overpotential, accepting the proposed equivalent circuit structures presented in Table 1. The models were able to support reasonable fitting accuracy (as indicated by the weighted sum of squared errors) across all the MEA configurations.

Both the aggregated electrolyte resistance (*Re*) and the charge transfer/polarization resistance (*Ret*) were reduced by the use of CEM as were the diffusional overpotentials represented by the GWF element parameters (A_{Wo}, p and τ). Hydrogel in its drier state reduced *Ret* but slightly increased *Re*. From Fig. 5 it is evident that fresh undried hydrogel, as a component of the MEA, is able to improve the MFC's performance by considerably reducing $|Z|$ and phase lag at low frequency, which is most relevant to the MFC, typically operating almost at d.c. conditions. When the water content of the hydrogel was reduced by drying, an increase in *Re* was observed and may be associated with an increased resistance to ionic current through the MEA. However, a higher level of hydration appeared to increase the capacitance of the system to the point that it was no longer the limiting factor in the open circuit EIS of the MFC and the diffusion model needed to be changed to Model-B (Table 1). The degree of hydration is likely to affect contact with cathode catalyst and transport of ionic species to the cathode. Control and matching of load and internal impedance along with appropriate control of hydrogel hydration could further improve MEA performance by providing optimal contact and ion conductivity.

Water formation by oxygen reduction on the cathode has been known to be insufficient to maintain a moist cathode in a membrane electrode assembly MFC [28]. However it might be resolved in MEA MFCs because they intrinsically contain a liquid medium in the anode chamber and liquid could be transported through the membrane by hydrostatic and osmotic pressure. This liquid transport could be accompanied by ionic species/proton migration which sustains the oxygen reduction reaction on the cathode. Cathode hydration might be particularly important in large scale bioreactor type MFCs which employ permeable separators such as membranes (or suitable material to maintain containment and mechanical integrity), in comparison to a compact chemical fuel cell. In addition, our study suggests that the water from the anode chamber is forced to move to the cathode by electro-osmotic drag induced by ionic species transport from the electrochemical reaction [14]. Therefore, the aggregated water transport through the membrane maintains wetness and humidity and consequently sustains ion transport and the cathode electrochemical reaction. Further study will be required to investigate a separator material which facilitates ion transport and alleviates possible high localized pH on the cathode while maintaining containment and mechanical integrity [30], and also improves MFC performance.

MFCs have evolved from their early stage of small scale bottle or cube MFCs into tubular type reactors [17,31,32]. This trend may reflect the fact that MFC design is progressing toward bioreactor configurations, and that scaled wastewater treatment systems could be a good stepping stone for the advancement of MFC technology [1,2,33]. Scale-up is an important issue in MFC design. The reactor configuration reported in this paper might be feasible for continuous treatment of organic wastewater requiring large volume systems. Modules of tubular MFCs employing MEAs could be physically extended by a combination of multiple tubular reactors to increase aspect ratio, but evidence is needed to show that the power production is usefully commensurate. Recent progress of anode design for increasing surface area and retention (e.g. brush anode electrode) [27] could be combined with MEAs to accomplish efficient wastewater treatment as well as energy recovery.

5. Conclusions

Low cost ion exchange membrane and polypropylene tubing can be used in the construction of batch fed, high aspect ratio, air cathode tubular MFCs to yield power densities of 6.1 $W m^{-3}$, despite their relatively large (200 cm^3 empty bed anode) volume and MEA area for oxygen diffusion (228 cm^2). This MFC configuration was able to achieve high coulombic efficiencies, reaching 71%. A comparison between cation and anion exchange membranes as mechanically assembled MEAs, with and without a hydrogel as a filler material between the membrane and cathode, showed that the MFC using CEM with hydrogel exhibited the highest power density. EIS in association with equivalent circuit models can be used to investigate the functional morphology and suggest reduced impedance and enhanced membrane–cathode contact area when hydrophilic gel was applied to the membrane. The net water loss through the membrane varied according to external load resistance due to electro-osmotic drag. The MEA developed here has been shown to be mechanically robust, operating for more than 6 months at this scale without problems.

Acknowledgements

This research was funded by the UK EPSRC SUPERGEN Biological Fuel Cell project (EP/D047943/1) supported by grant 68-3A75-3-150. The authors thank Dr. Steve Tennison of MAST Carbon Technology Ltd. for providing activated monolith carbon.

References

[1] B.E. Logan, J.M. Regan, Environ. Sci. Technol. 40 (2006) 5172–5180.
[2] B.E. Rittmann, Trends Biotechnol. 24 (2006) 261–266.
[3] B. Min, B.E. Logan, Environ. Sci. Technol. 38 (2004) 5809–5814.
[4] B. Min, J.R. Kim, S. Oh, J.M. Regan, B.E. Logan, Water Res. 39 (2005) 4961–4968.
[5] H. Liu, B.E. Logan, Environ. Sci. Technol. 38 (2004) 4040–4046.
[6] Y. Fan, H. Hu, H. Liu, Environ. Sci. Technol. 41 (2007) 8154–8158.
[7] J.C. Biffinger, R. Ray, B. Little, B.R. Ringeisen, Environ. Sci. Technol. 41 (2007) 1444–1449.
[8] Y. Zuo, S. Cheng, D. Call, B.E. Logan, Environ. Sci. Technol. 41 (2007) 3347–3353.
[9] S. You, Q. Zhao, J. Zhang, J. Jiang, S. Zhao, J. Power Sources 162 (2006) 1409–1415.
[10] B. Kim, I. Chang, G. Gadd, Appl. Microbiol. Biotechnol. 76 (2007) 485–494.
[11] B. Tartakovsky, S.R. Guiot, Biotechnol. Prog. 22 (2006) 241–246.
[12] H. Liu, S. Cheng, L. Huang, B.E. Logan, J. Power Sources 179 (2008) 274–279.
[13] Y. Fan, H. Hu, H. Liu, J. Power Sources 171 (2007) 348–354.
[14] J. Larminie, A. Dicks, Fuel Cell Systems Explained, second ed., J. Wiley, Chichester, West Sussex, 2003.
[15] T.H. Pham, J.K. Jang, H.S. Moon, I.S. Chang, B.H. Kim, J. Microbiol. Biotechnol. 15 (2005) 442–446.
[16] J.R. Kim, S. Cheng, S.E. Oh, B.E. Logan, Environ. Sci. Technol. 41 (2007) 1004–1009.
[17] K. Rabaey, P. Clauwaert, P. Aelterman, W. Verstraete, Environ. Sci. Technol. 39 (2005) 8077–8082.
[18] A. Giuffrida, Heterogeneous membrane and method, International Patent WO9406850, 1994.
[19] Z. He, N. Wagner, S.D. Minteer, L.T. Angenent, Environ. Sci. Technol. 40 (2006) 5212–5217.
[20] S. Cheng, H. Liu, B.E. Logan, Environ. Sci. Technol. 40 (2006) 364–369.
[21] H. Liu, S. Cheng, B.E. Logan, Environ. Sci. Technol. 39 (2005) 5488–5493.
[22] E. Katz, I. Willner, Electroanalysis 15 (2003) 913–947.
[23] D.R. Franceschetti, J.R. Macdonald, R.P. Buck, J. Electrochem. Soc. 138 (1991) 1368–1371.
[24] K. Yamada, K. Yasuda, N. Fujiwara, Z. Siroma, H. Tanaka, Y. Miyazaki, T. Kobayashi, Electrochem. Commun. 5 (2003) 892–896.
[25] G.Q. Lu, F.Q. Liu, C.-Y. Wang, Electrochem. Solid-State Lett. 8 (2005) A1–A4.
[26] J.R. Kim, S.H. Jung, J.M. Regan, B.E. Logan, Bioresour. Technol. 98 (2007) 2568–2577.
[27] B. Logan, S. Cheng, V. Watson, G. Estadt, Environ. Sci. Technol. 41 (2007) 3341–3346.
[28] K. Rabaey, G. Lissens, W. Verstraete, Biofuels for Fuel Cells: Biomass Fermentation Towards Usage in Fuel Cells, IWA Publishing, London, 2005.
[29] H. Liu, S. Cheng, B.E. Logan, Environ. Sci. Technol. 39 (2005) 658–662.
[30] F. Zhao, F. Harnisch, U. Schroder, F. Scholz, P. Bogdanoff, I. Herrmann, Environ. Sci. Technol. 40 (2006) 5193–5199.
[31] S. You, Q. Zhao, J. Zhang, J. Jiang, C. Wan, M. Du, S. Zhao, J. Power Sources 173 (2007) 172–177.
[32] K. Scott, C. Murano, G. Rimbu, J. Appl. Electrochem. 37 (2007) 1063–1068.
[33] K. Rabaey, W. Verstraete, Trends Biotechnol. 23 (2005) 291–298.
[34] E. Barsoukov, J.R. Macdonald, Impedance Spectroscopy: Theory, Experiment, and Applications, second ed., Wiley, New York, 2005.